

Interaction of Acetonitrile with Water-Ice: An Infrared Spectroscopic Study

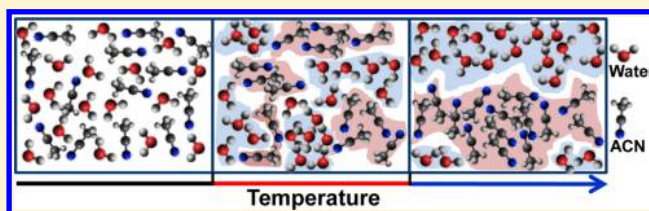
Radha Gobinda Bhuin,^{†,§} Rabin Rajan J. Methikkalam,^{†,§} Bhalamurugan Sivaraman,[‡] and Thalappil Pradeep^{*,†}

[†]DST Unit of Nanoscience (DST UNS) and Thematic Unit of Excellence (TUE), Department of Chemistry, Indian Institute of Technology Madras, Chennai 600 036, India

[‡]Space and Atmospheric Sciences Division, Physical Research Laboratory, Ahmedabad, India

S Supporting Information

ABSTRACT: Interaction of water-ice and acetonitrile has been studied at low temperatures in their codeposited mixtures, in ultrahigh vacuum conditions. They interact strongly at low temperatures (in the temperature range of 40–110 K), which was confirmed from the new features manifested in the reflection absorption infrared spectra of the mixtures. This interaction was attributed to strong hydrogen bonding which weakens upon warming as the acetonitrile molecules phase segregate from water-ice. Complete phase separation was observed at 130 K prior to desorption of acetonitrile from the water-ice matrix. Such a hydrogen-bonded structure is not observed when both the molecular solids are deposited as water on acetonitrile or acetonitrile on water overlayers. A quantitative analysis shows that in a 1:1 codeposited mixture, more than 50% acetonitrile molecules are hydrogen bonded with water-ice at low temperatures (40–110 K).



1. INTRODUCTION

Water-ice is omnipresent in its amorphous form. Studying interactions of different molecules with water-ice is of tremendous interest as it would lead to an understanding of amorphous ice and of various phenomena of environmental and biological importance.¹ These interactions may be physical (as in absorption/adsorption² and trapping³) or chemical⁴ in nature. The latter is the case when water-ice acts as a catalyst to accelerate chemical reactions on its surface or when it participates in a reaction leading to the formation of new chemical species. Such interactions are influenced by the morphology and structure of water-ice.^{5–7} A representative example is the production of dihydrogen via the surface recombination of hydrogen atoms adsorbed on amorphous ice.⁸ Several physical phenomena like adsorption/desorption kinetics,^{2,6} diffusion,^{2,9} and trapping³ are also highly dependent on the morphology of water-ice. Porous amorphous ice can trap several small molecules inside its pores, which can only be released when it undergoes a structural change.

Various factors including local temperature,¹⁰ incident flux,¹¹ incident angle,¹² and kinetic energy¹³ affect the morphology of water-ice. Morphology of water-ice generated by vapor deposition on a cold surface is substantially dependent on temperature. Crystallization and morphological change of amorphous ice has been studied extensively.^{14–16} At temperatures below 120 K vapor deposition, it is known to form amorphous ice.¹⁷ Several studies have revealed that amorphous ice so formed upon heating undergoes a structural change at ~120 K, before crystallizing at ~140 K.^{18,19} Thus, interactions of molecules with water-ice are expected to be temperature-

dependent and are likely to change as it goes through different structural modifications.

A number of factors make acetonitrile (ACN), a very important molecule. The vibrational spectrum of ACN is well-understood in the gas, liquid, and solid phases, and its interaction with a variety of molecules is also well-characterized.^{20–23} ACN is the simplest nitrile and is extensively used in organic syntheses because of its ability to dissolve a wide range of ionic and nonpolar molecules. This makes it a model organic system. The study of interactions of ACN with water-ice is important and is relevant to the Interstellar medium (ISM). Literature is therefore rich in studies of ACN–water systems, examining their gas, liquid, and solid phase interactions.^{20,24–34} It is now known that interaction of ACN with water is mainly due to hydrogen bond formation. In the following section, we present the current understanding of the water–ACN system.

ACN and water systems have been studied extensively.^{25,26,31–34} However, most of the studies were performed on solutions,^{27,31,32,34} a few exist on solid films as well.^{1,24,35} Various studies have been carried out with water and acetonitrile mixtures in the liquid phase.^{31,32,36} Experiments were performed by varying the mole fraction of the components in the mixtures, and studies suggest the formation of different microstructures of the mixtures. A molecular dynamics study proposed a microheterogeneous structure at

Received: December 18, 2014

Revised: May 4, 2015

Published: May 4, 2015

sufficiently high acetonitrile content.³⁷ In such a structure, clusters of one type of molecules are formed (i.e., either of ACN or H₂O and at low ACN content water structure become more ordered). Radial distribution functions of $g_{O-O}(r)$ (O denotes the oxygen of water) significantly increases for 88% ACN solution compared to pure water, which suggests the formation of water clusters. Comparison of $g_{O-O}(r)$ of 12% ACN solution and pure water shows an enhancement of the water structure in the former. On the contrary, Raman spectroscopic study of the CD₃CN–H₂O–HDO system did not support enhancement of the water structure, whereas at intermediate compositions formation of clusters was evident.³⁴ The OH and CN stretching bands in the spectra were monitored for this investigation. However, IR investigation by Gorbunov and Naberukhin was unable to suggest the existence of clusters at any concentration.³⁸ A detailed experimental and theoretical study revealed that microheterogeneity begins above $x_{ACN} = 0.22 \pm 0.11$, and at low concentration, ACN is solvated by H₂O.³⁹ A transmission IR study of ACN–H₂O showed the interaction of ACN with H₂O at different mole fractions. In this, C≡N stretching mode of the CD₃CN–H₂O mixture and OD stretching mode of dilute HDO in the CH₃CN–H₂O mixture were monitored at 20 °C. From a Lorentzian fit of the C≡N band for different mixtures, the percentage of H-bonded ACN has been predicted.³¹ Attenuated total reflection (ATR) spectroscopy was also used to calculate the fraction of H-bonded ACN in the ACN–H₂O mixtures.³² Different compositional mixtures were studied, and the integrated intensity of C≡N stretching band were used to analyze the results. From these studies, it has been revealed that both free and H-bonded ACN molecules coexist in the mixture. Number of H-bonded ACN molecules in the mixture depends on their composition of mixing. Amount of free acetonitrile molecules is constant over a range of acetonitrile concentrations in the acetonitrile–water mixture ($0.7 \leq x_{ACN} \leq 1.0$).³⁶ Another study shows that free acetonitrile molecules present in the acetonitrile–water mixture are not affected by other water molecules, and they survive in the same environment as in pure ACN.³² ACN molecules in the ACN–H₂O mixture formed three-dimensional clusters, and the clusters are surrounded by the water molecules through H-bonding and dipole–dipole interactions.³⁶ Several different models are used to analyze the type and extent of interactions.^{31,32} Ab initio calculations of the ACN–H₂O system has also been performed.³³ In this study, the interaction of water monomer and clusters with the nitrile group has been discussed well. C≡N stretching frequencies for isolated ACN and ACN–water cluster have been calculated. In an ACN–water cluster, isolated ACN molecules were used to form the cluster with one or more water molecules. It was shown that ACN forms σ - and π -type H-bonds with water molecules. σ -Type H-bonded ACN shows a blue shift, whereas the π -type H-bonded ACN shows a red shift in C≡N frequencies. Interaction of ACN with a thin film of water has also been studied.^{20,24} As mentioned earlier, ACN can bind to the free OH/OD groups on the surface through hydrogen bonding or it can purely physisorb on the water-ice surface.^{20,24} Such an H-bonded ACN shows a blue shift in the C≡N stretching frequency.²⁴ Studies show that from the exposures of acetonitrile, presence of free OH group on the surface has been measured quantitatively. The peak appearing at 2264 cm⁻¹ for ACN-*h*₃:H₂O has been attributed to hydrogen-bonded ACN-*h*₃.²⁰ There is no evidence of formation of the hydrogen bond with crystalline ice.²⁰

Although there has been many reports on water–ACN interaction in solution and solid phases, until today there is no such report where interaction of both the molecules is studied in their codeposited mixture. In this paper, we have studied the interaction of ACN molecules with water-ice in their codeposited mixture. Acetonitrile and water were codeposited on a cold surface in order to mimic the ISM conditions. For comparison, layer-on-layer deposited ACN and water-ice systems were also examined. The interaction of the two species was analyzed through reflection absorption infrared spectroscopy, and the effect of temperature was investigated. The distinct difference between codeposited mixtures and overlayer deposition is brought out in these studies.

2. EXPERIMENTAL SECTION

The experimental setup used for this study is given in more detail elsewhere.⁴⁰ The instrument consists of three chambers; namely, the ionization chamber, the octupole chamber, and the scattering chamber. Each chamber was differentially pumped by turbomolecular pumps backed by diaphragm pumps. Base pressure of the instrument was 5.0×10^{-10} mbar, and the pressure was $\sim 2.0 \times 10^{-9}$ mbar during the experiment. Though the chamber has several facilities for probing molecular solids, we have used only a reflection absorption infrared spectrometer (RAIRS), a quadrupole mass spectrometer, and a low-energy alkali ion gun in the study presented here. A Bruker VERTEX 70 FT-IR spectrometer was used to measure the spectra, with external optics, which has been fully described elsewhere.⁴⁰ The spectrometer resolution for the studies reported has been set at 2 cm⁻¹. To describe the experiment, briefly, the substrate is a Ru(0001) single crystal attached at the tip of a closed cycle helium cryostat on a copper holder, fitted with a resistive heater. The substrate can be maintained at any temperature between 8 and 1000 K. The temperature is measured by employing a thermocouple sensor with an accuracy of 0.001 K. Repeated heating at 1000 K ensures surface cleanliness. The temperature ramping is controlled and monitored by a temperature controller (Lakeshore 336). In this work, we have used a temperature window of 40–200 K to investigate the interaction of our ACN–water-ice systems. Temperatures in the range of 40–80 K were tested initially, but significant differences in the IR spectra were not observed. Therefore, in the proceeding experiments, only the temperature range of 80–160 K was examined, in which the IR peaks of the ACN–water-ice system showed a large change.

As received, 99.95% pure acetonitrile (named as ACN-*h*₃) and its deuterated form (named as ACN-*d*₃), both from Sigma-Aldrich, H₂O (Millipore; 99.996%) and D₂O (99.995% purity, Sigma-Aldrich) were further purified by several freeze pump thaw cycles. The above liquids were filled in a glass-to-metal seal adapter tubes fitted in two different sample lines and were connected to a rotary pump. The sample lines were evacuated, the liquid was evaporated, and the vapors were deposited onto the precooled Ru(0001) substrate using all-metal leak valves. The various samples, namely, ACN layer over H₂O layer, H₂O layer over ACN layer, and codeposited ACN and H₂O are referred to as H₂O@ACN, ACN@H₂O, and ACN:H₂O, respectively. For both the deposition techniques, two separate sample gas lines connected with two separate leak valves were used to avoid mixing of vapors in the sample line itself. During deposition, the mass spectral intensity from the quadrupole mass spectrometer was used to calculate the ratio of ACN to water in the mixture. We have consistently kept a 1:1 ratio of

the two in each system. All the samples were deposited on the precooled ruthenium single crystal substrate at 40 K and gradually heated (at a ramping rate of 1 K min^{-1}) to a series of temperatures to collect the temperature-dependent IR spectra. On reaching a particular temperature, the spectrum was collected after a short gap of 3 min to equilibrate the temperature. The 1 K min^{-1} slow ramping rate helped us to ensure that the temperature change before and during the spectral collection was not significant and was within $\pm 0.02 \text{ K}$. Each spectrum was obtained by averaging 512 scans, with a resolution of 2 cm^{-1} . The large number of scans ensured that the signal-to-noise ratio was high.

Cs^+ ion (m/z 133) is a well-known projectile for secondary ion mass spectrometry.⁴¹ Cs^+ ion scattering is a good technique to characterize solid samples deposited on a substrate at low temperatures. We have performed ion collision experiments using Cs^+ ions of 1 keV energy generated from a low-energy alkali ion gun (Kimball Physics Inc., IGPS-1016B). These ions were focused to collide at a specific energy on the codeposited acetonitrile water-ice system. The resulting scattered ions were analyzed using a quadrupole mass analyzer fitted on the ion-scattering chamber.

3. RESULTS

We began our investigation by first measuring the temperature-dependent RAIR spectra of $\text{ACN-}h_3$. For this, approximately 500 monolayers (ML) (assuming $1 \text{ ML} = 1 \times 10^{15}$ number of molecules/ cm^2) of $\text{ACN-}h_3$ were deposited on Ru(0001) at 40 K, and its IR spectrum was measured at different temperatures. The RAIR spectra in the 80 to 135 K range are shown in Figure 1. The spectrum at 80 K shows the presence of almost all the

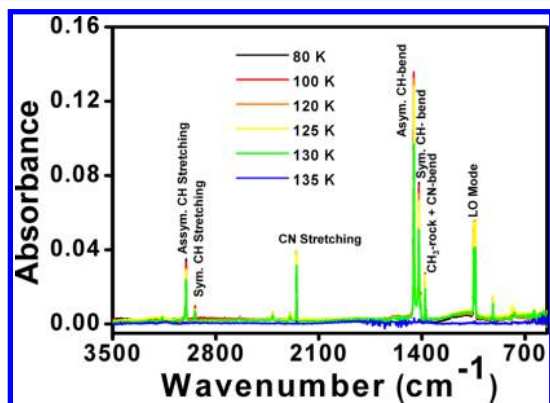


Figure 1. Temperature-dependent RAIRS spectra of pure ACN. 500 ML of ACN was deposited on a cold Ru(0001) surface at 40 K and heated to 135 K, and IR spectra were collected at different temperatures.

vibrational modes and is in good agreement with the reported RAIRS spectrum of pure $\text{ACN-}h_3$ at 110 K.⁴² It is also noticeable from the figure that (a) there is no spectral change until 130 K, (b) an intensity loss occurs at 130 K as the $\text{ACN-}h_3$ molecules start desorbing from the surface, and (c) the desorption is complete at 135 K.

For studying the interaction of water and acetonitrile molecules, they were codeposited in a 1:1 ratio on a ruthenium substrate at 40 K to form different ice samples. These were subsequently heated up to 160 K, which is the desorption point of water, and the IR spectrum was collected at various temperatures. The spectra at temperatures between 40 and 80

K were similar in appearance, and therefore, in the figures we show only those at 80 K for clarity. In order to understand the changes in the IR peaks at different temperatures more clearly, we used combinations of $\text{ACN-}h_3$ and $\text{ACN-}d_3$ with H_2O and D_2O .

The full RAIRS spectra for $\text{ACN-}h_3\text{:H}_2\text{O}$ at different temperatures are provided in Figure S1 of the Supporting Information. Figure 2a shows the O–H stretching region for

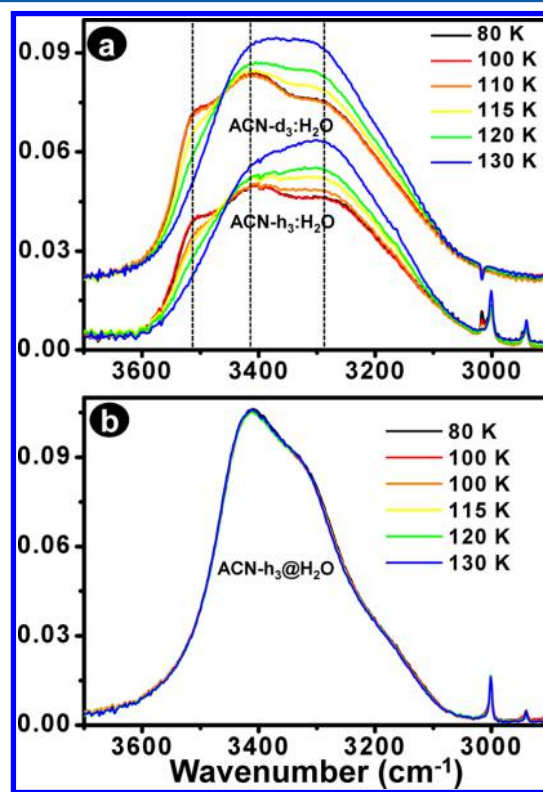


Figure 2. Temperature-dependent RAIRS spectra in the OH stretching region of (a) 1:1 codeposited $\text{ACN-}h_3\text{:H}_2\text{O}$ and $\text{ACN-}d_3\text{:H}_2\text{O}$ and (b) layer-on-layer $\text{ACN-}h_3\text{@H}_2\text{O}$ on cold Ru(0001) surface at 40 K.

$\text{ACN-}h_3\text{:H}_2\text{O}$ and $\text{ACN-}d_3\text{:H}_2\text{O}$. Three bands centered at 3510, 3415, and 3290 cm^{-1} are clearly noticeable at 80 K, and their peak positions are highlighted in the figure by dashed lines. The bands arise due to the interaction of acetonitrile and water and steadily disappear as the temperature increases beyond 115 K, eventually becoming a broad peak centered at $\sim 3350 \text{ cm}^{-1}$ that is characteristic of pure water-ice at 130 K. These observations can be understood as follows. In our $\text{ACN:H}_2\text{O}$ mixture, water can participate in H-bonding with acetonitrile when the free O–H group of water and the $\text{C}\equiv\text{N}$ group of ACN are in close proximity. The bonding is strong at low temperatures but gets weakened with an increase in temperature. At this stage, ACN molecules probably phase segregate from the water molecules while staying within the water matrix. Complete phase segregation takes place above 130 K where molecular motion of ACN is sufficiently high. Compared to pure ACN on Ru(0001), a relatively higher temperature is needed for ACN to desorb from the water matrix, and complete desorption occurs only during crystallization of water above 140 K.

The next set of experiments was performed for $\text{ACN-}h_3\text{@H}_2\text{O}$, and an enlarged view of the O–H stretching region of the RAIRS spectra is presented in Figure 2b (for complete spectra

see Figure S2 of the Supporting Information). Only a broad absorption feature of O–H stretching centered at $\sim 3400\text{ cm}^{-1}$ is observed at all the temperatures. It is clearly visible that the spectra from 80 to 130 K overlap with each other. The three bands seen in the case of ACN- h_3 :H $_2$ O are absent here. Thus, we expect little-to-no interaction between ACN and water molecules in this case compared to the previous experiment. Similar to the codeposited system, ACN- h_3 starts desorbing from the surface at 140 K when water undergoes crystallization and leaves it completely at 145 K. Crystallization of water was clearly seen in the spectra (see Figure S2 of the Supporting Information).

As a next set of experiments, ACN- h_3 :H $_2$ O was collided with 1 keV Cs $^+$ ions at 40 K and a typical mass spectrum (MS) is plotted in Figure 3. Species which are present on the surface

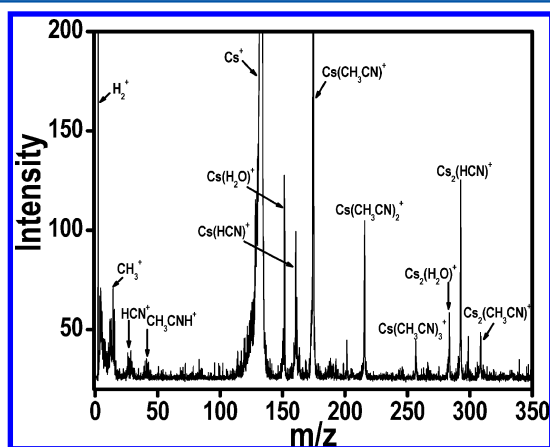


Figure 3. Mass spectrum of ACN- h_3 :H $_2$ O mixture obtained on 1 keV Cs $^+$ ion collision.

can be picked up by Cs $^+$ ions.⁴¹ The MS for ACN- h_3 :H $_2$ O contains peaks corresponding to adducts of Cs $^+$ ions with both H $_2$ O and ACN- h_3 , which indicates the coexistence of these two molecules on the Ru(0001) surface. The spectrum also shows the formation of the ACN dimer and trimer adducts with Cs $^+$ ions due to the high-energy impact of Cs $^+$ ions on the surface. It is possible that when ACN- h_3 and water were deposited together, both got uniformly mixed in the bulk and on the surface, and thus, the mass spectrum obtained shows the presence of both the species. But in mixtures where ACN is covered by water or water is covered by ACN, only one type of molecular species will be accessible to Cs $^+$ ions, which will therefore form adduct products only with the species that is present on the surface. Indeed when similar studies were performed for ACN- h_3 @H $_2$ O and H $_2$ O@ACN- h_3 systems (with thickness of each layer ~ 250 ML), Cs $^+$ ions formed adducts only with H $_2$ O and ACN- h_3 , respectively.

Figure 4a compares the C–H asymmetric (3000 cm^{-1}) and symmetric (2940 cm^{-1}) stretching regions of the RAIRS spectra of pure ACN- h_3 , ACN- h_3 :H $_2$ O, and ACN- h_3 @H $_2$ O. The spectral features of pure ACN- h_3 and ACN- h_3 @H $_2$ O were found to be quite similar, with two major peaks at 3000 and 2940 cm^{-1} . In the case of the ACN- h_3 :H $_2$ O system, an additional peak can be seen in both the C–H asymmetric and symmetric stretching regions (Figure 4a), though the former one is far more prominent. The new peak at $\sim 3017\text{ cm}^{-1}$ visible at 80 K gradually disappeared upon heating. This peak may have arisen due to the interaction of the C–H bond of

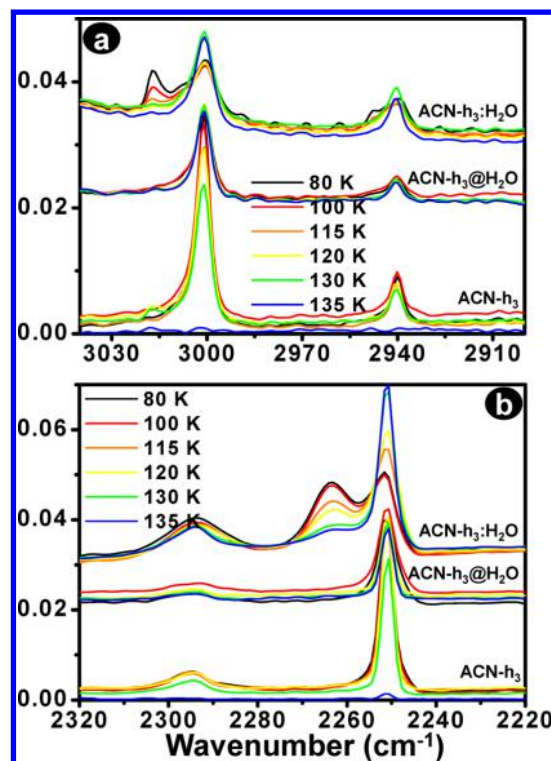


Figure 4. (a) Enlarged view of C–H asymmetric and symmetric stretching regions and (b) C \equiv N stretching region of ACN- h_3 of pure acetonitrile, ACN- h_3 :H $_2$ O, and ACN- h_3 @H $_2$ O at different temperatures.

ACN- h_3 with H $_2$ O. Interestingly, this feature was not present in the spectra for the ACN- h_3 @H $_2$ O system.

Figure 4b compares ACN- h_3 :H $_2$ O with pure ACN- h_3 and ACN- h_3 @H $_2$ O in the C \equiv N stretching region. It shows an extra peak for ACN- h_3 :H $_2$ O at $\sim 2264\text{ cm}^{-1}$ at 80 K whose intensity decreases as temperature is enhanced, and it vanishes completely at 130 K, similar to the disappearance of the bands in the O–H stretching region with a simultaneous regeneration of the H $_2$ O feature (Figure 2a). Simultaneous disappearance of the new bands in the O–H stretching region and of the peak at 2264 cm^{-1} with temperature suggests that the C \equiv N bond of ACN- h_3 could participate in bonding with H $_2$ O. However, it is also noted that the above-mentioned peak in the C \equiv N stretching region did not appear for ACN- h_3 @H $_2$ O. This confirms that the interaction between both the molecules takes place only when they are in good contact. An analysis of the temperature-dependent RAIRS spectra was also performed for the H $_2$ O@ACN- h_3 system (data not shown here), which showed that the trends are similar to ACN- h_3 @H $_2$ O. In this case, ACN- h_3 desorbed at 135 K, just like pure ACN- h_3 , prior to the crystallization of water.

The C–H bending region of the spectra for ACN- h_3 , ACN- h_3 @H $_2$ O, and ACN- h_3 :H $_2$ O is plotted in Figure 5a. The figure establishes that there is no change in the C–H bending region on going from pure ACN- h_3 to ACN- h_3 @H $_2$ O. But a significant change is observed when both the molecules are codeposited. The appearance of a new peak at 1444 cm^{-1} was seen, which slowly vanished upon heating, in a manner similar to the other regions. This further confirms the interaction of ACN- h_3 and H $_2$ O in ACN- h_3 :H $_2$ O.

In order to gain more insight into the interaction of ACN with water and changes in the IR peaks with temperature, H $_2$ O

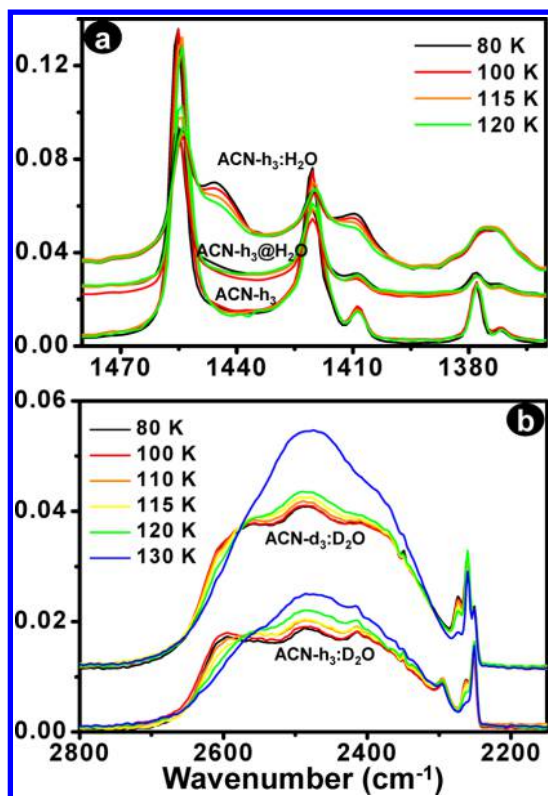


Figure 5. Temperature-dependent RAIRS spectra in (a) bending mode of C–H bond of ACN, ACN- h_3 :H $_2$ O, and ACN- d_3 :H $_2$ O mixtures and (b) O–D stretching mode of codeposited ACN- h_3 :D $_2$ O and ACN- d_3 :D $_2$ O mixtures.

was replaced by D $_2$ O, and mixtures of ACN- h_3 and ACN- d_3 with D $_2$ O were studied. Figure 5b displays the RAIRS spectra for codeposited 1:1 ACN- h_3 :D $_2$ O and ACN- d_3 :D $_2$ O mixtures at 40 K and, subsequently, heated to 130 K. The general features and trends are in good agreement with the ACN- h_3 :H $_2$ O interaction. For instance, there were no changes in the spectra between 40 and 80 K and so, only the spectrum at 80 K is shown. Here too, three peaks can be seen at 80 K, which continue to be noticeable until 120 K, and at 130 K, the pure O–D stretching is regained. However, for these systems, the C \equiv N stretching of acetonitrile overlaps with the broad band of O–D stretching. Figure 6a illustrates the C \equiv N stretching region of pure ACN- d_3 , ACN- h_3 :D $_2$ O, and ACN- d_3 :D $_2$ O at different temperatures. For pure ACN- d_3 , a doublet is observed with the two peaks positioned at 2250 and 2260 cm^{-1} . But a new peak emerges at 2274 cm^{-1} in the ACN- d_3 :D $_2$ O system, and it gradually disappears upon annealing (data for ACN- d_3 :H $_2$ O system is shown in Figure S3 of the Supporting Information). Comparing Figure 6a with Figure 4b, the variation of the C \equiv N stretching mode of ACN- h_3 :D $_2$ O with temperature is similar to that of ACN- h_3 :H $_2$ O. This confirms our earlier prediction that the interaction of acetonitrile and water occurs via a hydrogen bond between the C \equiv N group of acetonitrile and the OD/OH group of water. In Figure 6b, intensity of O–H stretching corresponding to the maximum peak position (as taken from the different codeposited systems) is plotted as a function of temperature. The figure shows that irrespective of the ACN:water system, the (a) intensity remains constant until 110 K, (b) starts increasing at 115 K, and (c) reaches a maximum at 130 K, beyond which desorption occurs.

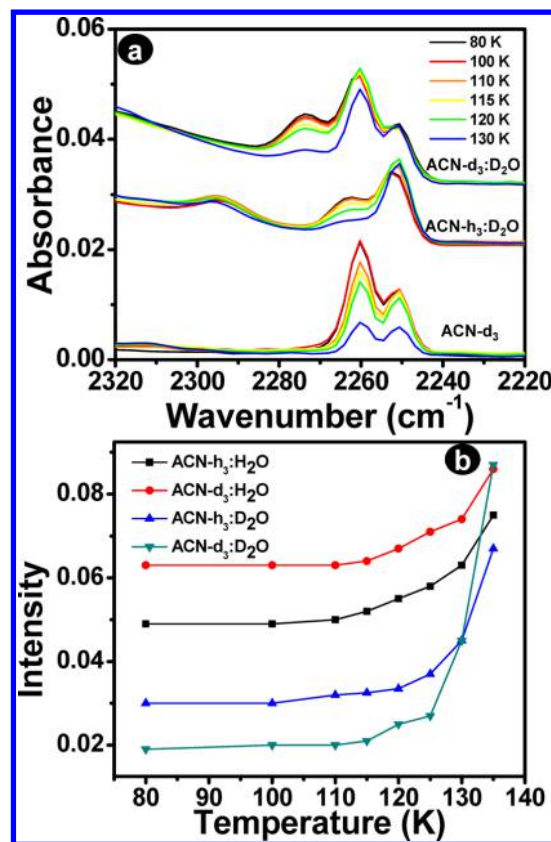


Figure 6. (a) C \equiv N stretching region of ACN- d_3 is shown at different temperatures for three different sets of ice samples. (b) Intensity of O–H stretching (maximum peak position) is plotted with respect to temperature.

4. DISCUSSION

From the data presented so far and in the light of earlier studies presented in the Introduction, let us now focus on the interaction of acetonitrile with water in the bulk ice phase. Strong interaction of codeposited acetonitrile and water at low temperatures (below 115 K) weakened as the temperature was increased. From all the experiments, it is evident that O–H/O–D bands of water and C \equiv N band of ACN are strongly affected by temperature. Three new bands appear in the O–H/O–D stretching region (Figure 2a) due to the interaction of ACN and water via H-bonding. These bands are retained until 110 K but start disappearing at 115 K and vanish completely at 130 K. The H-bonded C \equiv N stretching peak (2264 cm^{-1} for ACN- h_3 and 2274 cm^{-1} for ACN- d_3) starts decreasing in intensity at 115 K, which is reduced to zero at 130 K. From an ab initio study, it has been predicted that if ACNs form a σ -type H-bond, the C \equiv N stretching frequency is blue-shifted by 11.2 cm^{-1} , whereas when it forms the ACN-(H $_2$ O) $_3$ cluster, the C \equiv N stretching frequency is blue-shifted by 24.3 cm^{-1} .³³ We have also observed blue shifts in the C \equiv N frequencies which imply the formation of the σ -type H-bond between ACN and water. However, it was not possible to estimate the exact number of water molecules interacting with one molecule of ACN. In our study, we have seen an \sim 13 cm^{-1} blue shift in the H-bonded C \equiv N stretching frequency from the free C \equiv N stretching frequency irrespective of the samples. In general, calculated IR values do not match exactly with the peak positions obtained in experiments carried out at low temperatures. However, from this observation, we may say that approximately one ACN

molecule is interacting with one water molecule. Interaction of ACN molecules with water-ice is highly temperature sensitive, particularly in the temperature range of 115–130 K, which is evident from the gradual changes in the peak intensity of newly formed peaks in the O–H stretching region and H-bonded peak in the C≡N stretching region.

In our codeposited mixtures, ACN and water were in a 1:1 ratio which allow more ACN molecules to come in direct contact with free OH groups to form hydrogen bonds. The system is quite similar to liquid phase mixing where both the species can mix homogeneously. Here also, both H-bonded and free ACN molecules coexist at temperatures below 115 K, which is evident from the C≡N stretching frequency. C≡N stretching frequency for both free and H-bonded ACN coexist in the codeposited mixture at low temperature (<115 K) and upon increasing the temperature, the H-bonded peak disappears (130 K) and intensity of the free ACN peak shows an increase. At an elevated temperature of ~115–120 K, their molecular motions increase, and the H-bonds between acetonitrile and water-ice weaken, causing phase segregation of ACN molecules from the mixture inside the matrix which completes at 130 K. So at temperatures above 115 K, the intermolecular H-bonding weakens, and H₂O–H₂O and ACN–ACN interactions are enhanced, leading to phase segregation. The phase segregation is evident from the simultaneous disappearance of the bands in the OH stretching region and the peaks in the stretching region of C≡N. Interestingly, phase segregation starts at the same temperature (115 K) and completes at 130 K for the different combinations of ACN (ACN-*h*₃ and ACN-*d*₃) and water (H₂O and D₂O) in the mixture (see Figure 6b).

On the basis of the results obtained at different codeposited experiments, we propose a quantitative analysis. In this analysis, the C≡N stretching region of different mixtures are taken into consideration. We have seen that the C≡N stretching peak consists of both H-bonded and free ACN molecules. The peak was fitted with Lorentzians and the components are analyzed. Spectra at three different temperatures for ACN-*d*₃:H₂O are shown in Figure 7 where the two peaks, namely peak 1 and

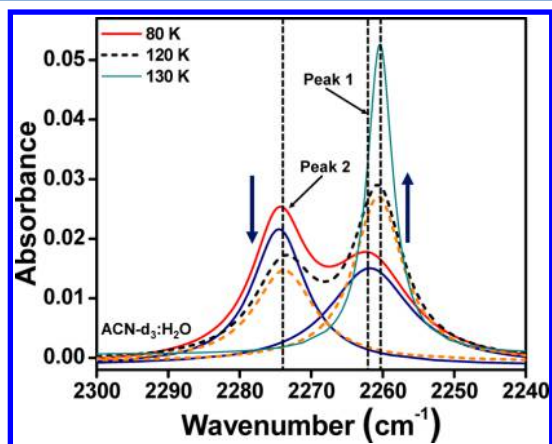


Figure 7. Lorentzian fit of the spectra of 1:1 ACN-*d*₃:H₂O at three different temperatures. Both fitted and cumulative spectra are shown in the figure. Two peaks in the cumulative spectra at each temperature are fitted with two components, peak 1 corresponds to the free ACN molecules and peak 2 corresponds to H-bonded ACN molecules. Fitted spectrum and cumulative spectrum were overlapping at 130 K. Hence, only fitted spectrum is shown in the figure at 130 K.

peak 2 are attributed to contributions from free and H-bonded ACN molecules. Areas of both the peaks are calculated and, from these, a fraction of H-bonded ACN molecules is calculated. A sum of the areas of peaks 1 and 2 gives the contribution due to total number of ACN molecules. Area of peak 2 is divided by the total area, which gives the fraction of H-bonded ACN molecules. This calculation is performed for four different sets of codeposited mixtures at different temperatures. Fraction of H-bonded molecules in different mixtures is plotted against temperature in Figure 8. In this

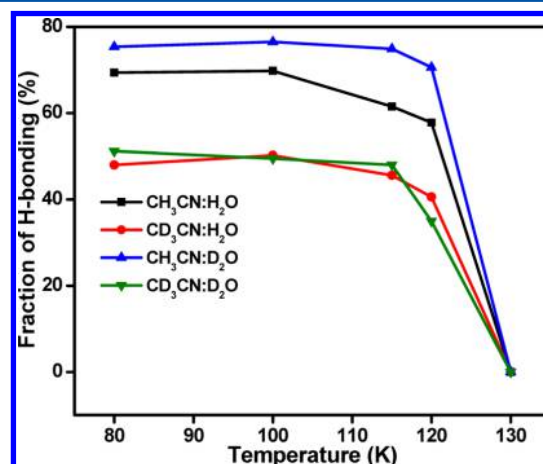


Figure 8. Fraction of H-bonded ACN molecules in different codeposited mixtures, plotted against temperature (see the text for details). Lines are drawn as to guide to eye and they do not represent a fit to the data.

calculation, we assume that once ACN molecules are phase-segregated from the mixture, no H-bonding exists. From the figure, it is evident that in all the different mixtures, more than 50% of ACN molecules are H-bonded with neighboring water molecules in the temperature range of 80–100 K. There is a sudden drop in the intensity of the H-bonded peak in the temperature range of 115–120 K, and finally it tends to zero at 130 K. Molecular motion of the species in the condensed phase is restricted. So the fraction of ACN molecules forming the H bond depends upon how the ACN molecules are oriented and how they are surrounded by H₂O molecules inside the ice matrix. This directly depends upon the concentration of both the molecules in the vapor phase during deposition. During deposition, we maintained the concentration as 1:1, which was closely monitored using a residual gas analyzer and, hence, we assume that the concentration of these molecules in the ice matrix is also 1:1. But it may not be an accurate assumption always as all the 1:1 codeposited mixtures may not give the same fraction of H bonding between ACN and water. More water molecules sitting near to ACN molecules leads to a higher number of H-bonding interaction between both the molecules. However, study reveals that in a 1:1 codeposited system, more than half of the ACN molecules are H-bonded with water molecules at low temperature (below 115 K). While this analysis is informative, it is only approximate. It is assumed that the cross sections of both the peaks (peaks 1 and 2) are the same and so their peak intensities are related to their respective concentrations by the same factor. We assume that interaction between the ACN and H₂O molecules is negligible at 130 K once they get phase segregated, which may not be true as ACN molecules are still in the water matrix and can interact, although

such interactions are weak or small in number to be seen by IR spectroscopy. Desorption of ACN near 135 K is disregarded. Another approach to doing a quantitative analysis is by using the infrared absorbance values along with TPD data. But that approach is not possible in our case due to experimental limitations.

From Figure 7, it is noticeable that free C≡N stretching frequency (peak 1) at 80 K is blue-shifted (shown in the figure by vertical lines) compared to the spectra at 120 and 130 K. Same data, with one more spectrum are shown in Figure S4 of the Supporting Information (spectrum at 100 K is not shown in Figure 7, for clarity). This observation indicates that strong interaction between both the molecules lead to the shift in free C≡N stretching frequency of ACN as well. When the molecules start segregating, the interaction is weakened, and free C≡N stretching frequency start appearing at the same position as in pure ACN.

The study confirms the formation of the H-bond between ACN and water-ice, and we have seen that both the molecules phase segregate above 130 K, where there is no or very limited H-bonding between them. We have also noticed that phase segregation starts at 115 K. But the mechanism of phase segregation remains unclear. To understand the mechanism of phase segregation we need to look at the structure of both the molecules at the temperature regime where phase segregation is occurring. It is reported that vapor deposited ACN at low temperature (below 115 K) is likely to form an amorphous phase with a randomly oriented structure, which on moderate annealing at 115 K initiates transitions to a crystalline phase.⁴³ The study indicates that ACN deposited at 100 K shows an unspecific broad intensity distribution in the XRD pattern, which is characteristic of amorphous structure of solid ACN. The same sample upon annealing to 115 K initiates a phase transition into a stable crystalline phase, which shows reflections in the diffractogram. Water vapor deposited below 120 K is amorphous, and ice undergoes a structural change at 120 K.^{18,19} In this structural transition, porous amorphous ice becomes nonporous at temperatures above 120 K, reducing the number of free OH groups in the process. Another study also revealed that amorphous ice undergoes a structural change of ~130 K before the onset of crystallization, leading to restrained amorphous ice.¹⁰ Other studies also revealed the structure of water-ice at different temperature. Laufer et al. suggested that amorphous ice exists at least in two different forms, one at <85 K and another at 85 < T < 136.8 K, before it undergoes crystallization.⁴⁴ Horimoto et al. also support the formation of microporous structure of amorphous ice, and it becomes pore free at 120 K.⁴⁵ So, all these studies suggest that in the temperature range of 115–130 K, both ACN and H₂O molecules undergo a structural change, which may be the force behind this phase segregation. This in turn starts at the temperature (115 K) where ACN undergoes crystallization. Crystallization leads to the increase in molecular motion. At the same time, amorphous ice also undergoes a structural change (120 K), where the microporous structure of amorphous ice is collapsed. This molecular motion of both the molecules affects the interaction between ACN and water-ice. This is clearly seen from Figure 9. In this figure (Figure 9), the maximum intensity of H-bonded and free C≡N stretching frequency of two different codeposited mixtures is plotted against temperature. The figure indicates that the intensity of both the peaks are constant until 110 K. At 115 K, the intensity of peak 2 shows a decrease and peak 1 shows an increase, which is indicating the

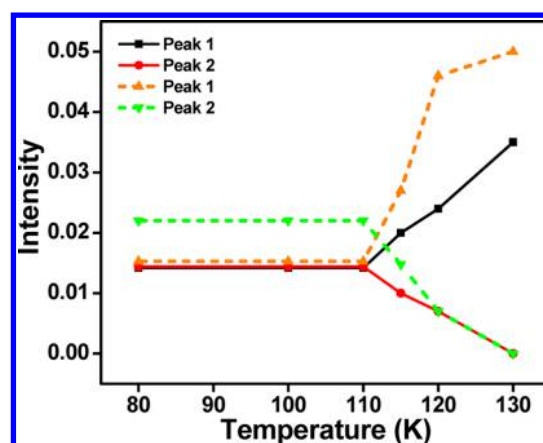


Figure 9. Maximum intensity of fitted (Lorentzian fit) free (peak 1) and H-bonded (peak 2) C≡N stretching frequency of ACN-*h*₃:H₂O (solid line) and ACN-*d*₃:H₂O (dotted line) is plotted against temperature.

breaking of the H-bond between ACN and water-ice. At 130 K, the intensity of peak 1 reaches maximum, whereas the intensity of peak 2 goes to minimum. A similar plot is shown in Figure 6b where maximum peak position of O–H/O–D is plotted against the temperature. This also indicates that the phase segregation starts at the same temperature (115 K) for all the codeposited mixtures. Phase segregation takes place well before the crystallization temperature of water-ice. Hence, nucleation of water-ice does not play any role in the phase segregation process.

Ample molecular motions of ACN at 130 K, where pure ACN starts desorbing from the surface, may also induce ACN molecules to segregate from the mixture. These phase segregated ACN molecules are covered with water-ice. As water-ice is nonporous in nature above 120 K, ACN may not be allowed to sit within the ice pores, rather it segregates to form a separate layer. In this layered structure, ACN molecules are overlaid by water molecules. We make this conclusion as desorption of ACN is not seen until 140 K. Infrared spectral features at high temperatures (above 130 K) also support a layered structure. During crystallization of water, water molecules reorient themselves and open a path for ACN molecules to desorb forming a molecular volcano. With an increase in temperature, there was no increase in pressure in the chamber, until the crystallization of water-ice where we have seen desorption of ACN. This observation indicates that desorption of ACN molecules takes place only when water molecules undergo crystallization.

Compared to ACN:H₂O, no spectral change was observed in the layer-on-layer-deposited ACN@H₂O as a function of temperature. This type of deposition does not allow proper mixing, and so water and ACN are not in 1:1 contact, as a result of which they are not able to form enough H bonds between them. There may be interfacial interaction in the overlayer deposited ACN@H₂O system, but we fail to observe it in our present measurement as we were probing the bulk ice, and hence, such interactions are much less seen by IR. The ACN@H₂O system is closer to the one after phase segregation has occurred (spectrum at 130 K in the ACN:H₂O system) from which ACN was desorbed completely at 145 K at the water crystallization temperature. Hence, we believe that cooling back a codeposited ACN:H₂O mixture after it has phase-separated above 120 K may act like an overlayer deposited ACN@H₂O

system, forming small islands of acetonitrile inside the water matrix with reduced interaction of ACN with water-ice.

Temperature-programmed desorption (TPD) spectroscopy is another way to study this interaction, particularly when molecules interact on the surface.^{20,46} TPD measurements of pure ACN-*h*₃, ACN-*h*₃:D₂O, and ACN-*h*₃@D₂O were performed, and comparison of the data is shown in Figure S5 of the Supporting Information. From the figure it is evident that pure ACN-*h*₃ desorb from the Ru(0001) surface with a peak maximum at ~132 K, whereas the other two cases desorption peak maximum appears above 140 K. Both the TPD spectra of the codeposited (ACN-*h*₃:D₂O) and sequential deposited (ACN-*h*₃@D₂O) systems behave in a similar fashion, which supports our argument that the codeposited system undergoes phase segregation and ACN get trapped inside the water-ice matrix, which is similar to the sequential deposited system. In the sequential deposition system, multilayer and monolayer peaks of ACN-*h*₃ are well-distinguished, but it is not prominent in the codeposited system. Desorption peak of ACN-*h*₃ in the codeposited system appears as a broad peak compared to the sequential deposition system which may be due to phase segregation in the codeposited system forming diffuse islands inside the water matrix. TPD can help to calculate the number of individual type of molecules present in the system. But in this study, it was not possible to measure TPD and RAIRS simultaneously.

5. CONCLUSIONS

The interaction of ACN–water-ice mixtures at low temperature has been studied using RAIRS spectroscopy. ACN and water were codeposited on a Ru(0001) substrate at 40 K and subsequently annealed to higher temperatures. The shifts in the IR peaks confirmed that (a) the molecular interaction between ACN and water-ice involved hydrogen bond formation, (b) the ACN molecules phase separate completely within the ice matrix at ~130 K, and (c) above 140 K, the water molecules reorient themselves causing the trapped ACN molecules to desorb. The study showed that in a 1:1 codeposited mixture of ACN and water-ice, more than 50% of ACN molecules participate in H-bonding with water-ice at a temperature below 115 K. Phase segregation is highly temperature-dependent in the temperature range of 100–130 K, and it is an irreversible process too. This explains how temperature-induced phase separation in an astronomical environment of similar ice mixtures can prevent the molecules from reacting with each other and thereby affect the kinetics of product formation.

Though there have been reports of irradiation processing of ACN–water mixtures, our results reveal the complexity of the interaction between the reacting molecules within the water-ices, which should be taken into account while studying other chemical reactions under similar conditions. Furthermore, the new spectral signatures recorded as a function of temperature may help astronomers to find the interacting molecules, rather than isolated ones in ISM and the atmosphere.

■ ASSOCIATED CONTENT

● Supporting Information

Temperature-dependent RAIR spectra of ACN-*h*₃:H₂O, ACN-*h*₃@H₂O, and ACN-*d*₃:H₂O system. Lorentzian fit of the spectra of 1:1 ACN-*h*₃:H₂O systems. TPD spectra of three different systems. This information is available from The Supporting Information is available free of charge on the ACS Publications website at DOI: 10.1021/jp512607v.

■ AUTHOR INFORMATION

Corresponding Author

*E-mail: pradeep@iitm.ac.in. Fax: + 91-44 2257-0545.

Author Contributions

§R.G.B. and R.R.J.M. contributed equally.

Notes

The authors declare no competing financial interest.

■ ACKNOWLEDGMENTS

T.P. acknowledges the Science and Engineering Research Board (SERB), Department of Science and Technology (DST), Government of India for research funding. R.G.B. thanks Council of Scientific and Industrial Research (CSIR), Government of India for a research fellowship. R.R.J.M. thanks the University Grant Commission (UGC) for his research fellowship. S.B. acknowledges the support from Physical Research Laboratory (PRL) and INSPIRE Grant (IFA-11CH-11).

■ REFERENCES

- (1) Schaff, J. E.; Roberts, J. T. Toward an Understanding of the Surface Chemical Properties of Ice: Differences between the Amorphous and Crystalline Surfaces. *J. Phys. Chem.* **1996**, *100*, 14151–14160.
- (2) Hama, T.; Watanabe, N. Surface Processes on Interstellar Amorphous Solid Water: Adsorption, Diffusion, Tunneling Reactions, and Nuclear-Spin Conversion. *Chem. Rev.* **2013**, *113*, 8783–8839.
- (3) Smith, R. S.; Huang, C.; Wong, E. K. L.; Kay, B. D. The Molecular Volcano: Abrupt CCl₄ Desorption Driven by the Crystallization of Amorphous Solid Water. *Phys. Rev. Lett.* **1997**, *79*, 909–912.
- (4) Cyriac, J.; Pradeep, T.; Kang, H.; Souda, R.; Cooks, R. G. Low-Energy Ionic Collisions at Molecular Solids. *Chem. Rev.* **2012**, *112*, 5356–5411.
- (5) Hornekaer, L.; Baurichter, A.; Petrunin, V. V.; Luntz, A. C.; Kay, B. D.; Al-Halabi, A. Influence of Surface Morphology on D₂ Desorption Kinetics from Amorphous Solid Water. *J. Chem. Phys.* **2005**, *122*, 124701-1–124701-11.
- (6) Ayotte, P.; Smith, R. S.; Stevenson, K. P.; Dohnalek, Z.; Kimmel, G. A.; Kay, B. D. Effect of Porosity on the Adsorption, Desorption, Trapping, and Release of Volatile Gases by Amorphous Solid Water. *J. Geophys. Res.* **2001**, *106*, 33387–33392.
- (7) Azria, R.; Le Coat, Y.; Lachgar, M.; Tronc, M.; Parenteau, L.; Sanche, L. Effects of Morphology in Electron-Stimulated Desorption: O⁻ from O₂ Condensed on D₂O Films Grown at 15–150 K on Pt. *Surf. Sci.* **1999**, *436*, L671–L676.
- (8) Roser, J. E.; Manico, G.; Pirronello, V.; Vidali, G. Formation of Molecular Hydrogen on Amorphous Water Ice. Influence of Morphology and Ultraviolet Exposure. *Astrophys. J.* **2002**, *581*, 276–284.
- (9) Cyriac, J.; Pradeep, T. Probing Difference in Diffusivity of Chloromethanes through Water Ice in the Temperature Range of 110–150 K. *J. Phys. Chem. C* **2007**, *111*, 8557–8565.
- (10) Jenniskens, P.; Blake, D. F. Structural Transitions in Amorphous Water Ice and Astrophysical Implications. *Science* **1994**, *265*, 753–756.
- (11) Smith, R. S.; Petrik, N. G.; Kimmel, G. A.; Kay, B. D. Thermal and Nonthermal Physicochemical Processes in Nanoscale Films of Amorphous Solid Water. *Acc. Chem. Res.* **2012**, *45*, 33–42.
- (12) Stevenson, K. P.; Kimmel, G. A.; Dohnalek, Z.; Smith, R. S.; Kay, B. D. Controlling the Morphology of Amorphous Solid Water. *Science* **1999**, *283*, 1505–1507.
- (13) Smith, R. S.; Zubkov, T.; Dohnalek, Z.; Kay, B. D. The Effect of the Incident Collision Energy on the Porosity of Vapor-Deposited Amorphous Solid Water Films. *J. Phys. Chem. B* **2009**, *113*, 4000–4007.

- (14) Backus, E. H. G.; Grecea, M. L.; Kleyn, A. W.; Bonn, M. Surface Crystallization of Amorphous Solid Water. *Phys. Rev. Lett.* **2004**, *92*, 236101-1–236101-4.
- (15) Kondo, T.; Kato, H. S.; Bonn, M.; Kawai, M. Morphological Change During Crystallization of Thin Amorphous Solid Water Films on Ru(0001). *J. Chem. Phys.* **2007**, *126*, 181103-1–181103-5.
- (16) Kondo, T.; Kato, H. S.; Bonn, M.; Kawai, M. Deposition and Crystallization Studies of Thin Amorphous Solid Water Films on Ru(0001) and on Co-Precovered Ru(0001). *J. Chem. Phys.* **2007**, *127*, 094703-1–094703-14.
- (17) Bag, S.; Bhuin, R. G.; Pradeep, T. Distinguishing Amorphous and Crystalline Ice by Ultralow Energy Collisions of Reactive Ions. *J. Phys. Chem. C* **2013**, *117*, 12146–12152.
- (18) Cyriac, J.; Pradeep, T. Structural Reorganization on Amorphous Ice Films Below 120 K Revealed by near-Thermal (~1 eV) Ion Scattering. *J. Phys. Chem. C* **2008**, *112*, 5129–5135.
- (19) Mate, B.; Rodriguez-Lazcano, Y.; Herrero, V. J. Morphology and Crystallization Kinetics of Compact (HGW) and Porous (ASW) Amorphous Water Ice. *Phys. Chem. Chem. Phys.* **2012**, *14*, 10595–10602.
- (20) Schaff, J. E.; Roberts, J. T. Interaction of Acetonitrile with the Surfaces of Amorphous and Crystalline Ice. *Langmuir* **1999**, *15*, 7232–7237.
- (21) Sexton, B. A.; Avery, N. R. Coordination of Acetonitrile (CH₃CN) to Platinum(111): Evidence for an H₂(C,N) Species. *Surf. Sci.* **1983**, *129*, 21–36.
- (22) Shannon, C.; Campion, A. Raman Spectroscopic Investigation of the Adsorption of Acetonitrile and Methanol on Silicon(100)-2 × 1. *Surf. Sci.* **1990**, *227*, 219–223.
- (23) Meijer, E. L.; van Santen, R. A.; Jansen, A. P. J. Computation of the Infrared Spectrum of an Acidic Zeolite Proton Interacting with Acetonitrile. *J. Phys. Chem.* **1996**, *100*, 9282–9291.
- (24) Bahr, S.; Kempter, V. Interaction of Acetonitrile with Thin Films of Solid Water. *J. Chem. Phys.* **2009**, *130*, 214509-1–214509-9.
- (25) Ahn, D.-S.; Lee, S. Density Functional Theory Study of Acetonitrile - Water Clusters: Structures and Infrared Frequency Shifts. *Bull. Korean Chem. Soc.* **2007**, *28*, 725–729.
- (26) Bako, I.; Megyes, T.; Palinkas, G. Structural Investigation of Water-Acetonitrile Mixtures: An Ab Initio, Molecular Dynamics and X-Ray Diffraction Study. *Chem. Phys.* **2005**, *316*, 235–244.
- (27) Kittaka, S.; Kuranishi, M.; Ishimaru, S.; Umahara, O. Phase Separation of Acetonitrile-Water Mixtures and Minimizing of Ice Crystallites from There in Confinement of Mcm-41. *J. Chem. Phys.* **2007**, *126*, 091103-1–091103-4.
- (28) Melnikov, S. M.; Hoeltzel, A.; Seidel-Morgenstern, A.; Tallarek, U. Adsorption of Water-Acetonitrile Mixtures to Model Silica Surfaces. *J. Phys. Chem. C* **2013**, *117*, 6620–6631.
- (29) Schaff, J. E.; Roberts, J. T. Adsorbed States of Acetonitrile and Chloroform on Amorphous and Crystalline Ice Studied with X-Ray Photoelectron Spectroscopy. *Surf. Sci.* **1999**, *426*, 384–394.
- (30) Zhang, D.; Gutow, J. H.; Eisenthal, K. B. Structural Phase Transitions of Small Molecules at Air/Water Interfaces. *J. Chem. Soc., Faraday Trans.* **1996**, *92*, 539–543.
- (31) Bertie, J. E.; Lan, Z. Liquid Water-Acetonitrile Mixtures at 25 °C: The Hydrogen-Bonded Structure Studied through Infrared Absolute Integrated Absorption Intensities. *J. Phys. Chem. B* **1997**, *101*, 4111–4119.
- (32) Jamroz, D.; Stangret, J.; Lindgren, J. An Infrared Spectroscopic Study of the Preferential Solvation in Water-Acetonitrile Mixtures. *J. Am. Chem. Soc.* **1993**, *115*, 6165–6168.
- (33) Choi, J.-H.; Oh, K.-L.; Lee, H.; Lee, C.; Cho, M. Nitrile and Thiocyanate Ir Probes: Quantum Chemistry Calculation Studies and Multivariate Least-Square Fitting Analysis. *J. Chem. Phys.* **2008**, *128*, 134506.
- (34) Kabisch, G. Raman Spectroscopic Studies on Water-Acetonitrile Mixtures. *Z. Phys. Chem.* **1982**, *263*, 48–60.
- (35) Dello Russo, N.; Khanna, R. K. Laboratory Infrared Spectroscopic Studies of Crystalline Nitriles with Relevance to Outer Planetary Systems. *Icarus* **1996**, *123*, 366–395.
- (36) Takamuku, T.; Tabata, M.; Yamaguchi, A.; Nishimoto, J.; Kumamoto, M.; Wakita, H.; Yamaguchi, T. Liquid Structure of Acetonitrile–Water Mixtures by X-Ray Diffraction and Infrared Spectroscopy. *J. Phys. Chem. B* **1998**, *102*, 8880–8888.
- (37) Kovacs, H.; Laaksonen, A. Molecular Dynamics Simulation and NMR Study of Water-Acetonitrile Mixtures. *J. Am. Chem. Soc.* **1991**, *113*, 5596–605.
- (38) Gorbunov, B. Z.; Naberukhin, Y. I. Structure of Aqueous Solutions of Nonelectrolytes Studied by Vibrational Spectroscopy. ii. Microstratification at Mean Concentrations. *Zh. Strukt. Khim.* **1975**, *16*, 816–25.
- (39) Marcus, Y.; Migron, Y. Polarity, Hydrogen Bonding, and Structure of Mixtures of Water and Cyanomethane. *J. Phys. Chem.* **1991**, *95*, 400–406.
- (40) Bag, S.; Bhuin, R. G.; Methikkalam, R. R. J.; Pradeep, T.; Kephart, L.; Walker, J.; Kuchta, K.; Martin, D.; Wei, J. Development of Ultralow Energy (1 - 10 eV) Ion Scattering Spectrometry Coupled with Reflection Absorption Infrared Spectroscopy and Temperature Programmed Desorption for the Investigation of Molecular Solids. *Rev. Sci. Instrum.* **2014**, *85*, 014103-1–014103-7.
- (41) Kang, H. Chemistry of Ice Surfaces. Elementary Reaction Steps on Ice Studied by Reactive Ion Scattering. *Acc. Chem. Res.* **2005**, *38*, 893–900.
- (42) Abdulgali, A. G. M.; Marchione, D.; Rosu-Finsen, A.; Collings, M. P.; McCoustra, M. R. S. Laboratory Investigations of Irradiated Acetonitrile-Containing Ices on an Interstellar Dust Analog. *J. Vac. Sci. Technol., A* **2012**, *30*, 041505-1–041505-6.
- (43) Tizek, H.; Grothe, H.; Knozinger, E. Gas-Phase Deposition of Acetonitrile: An Attempt to Understand Ostwald's Step Rule on a Molecular Basis. *Chem. Phys. Lett.* **2004**, *383*, 129–133.
- (44) Laufer, D.; Kochavi, E.; Bar-Nun, A. Structure and Dynamics of Amorphous Water Ice. *Phys. Rev. B* **1987**, *36*, 9219–9227.
- (45) Horimoto, N.; Kato, H. S.; Kawai, M. Stepwise Morphological Change of Porous Amorphous Ice Films Observed through Adsorption of Methane. *J. Chem. Phys.* **2002**, *116*, 4375–4378.
- (46) Burke, D. J.; Brown, W. A. Ice in Space: Surface Science Investigations of the Thermal Desorption of Model Interstellar Ices on Dust Grain Analogue Surfaces. *Phys. Chem. Chem. Phys.* **2010**, *12*, 5947–5969.